Available online at www.sciencedirect.com
SCIENCE DIRECT®
International Journal of Mass Spectrometry 228 (2003) 107–116
International Journal of Mass Spectrometry
www.elsevier.com/locate/ijms

Experimental studies on the formation of argon atoms in Ar^+–atoms collisions

H. Martínez[a,*], F. Castillo[b], P.G. Reyes[c], F.G. Santibañez[c]

[a] *Centro de Ciencias Físicas, UNAM, Apdo Postal 48-3, Cuernavaca Morelos 62251, Mexico*
[b] *Instituto Ciencias Nucleares, México. Distrito Federal, Mexico*
[c] *Facultad de Ciencias UAEMex, Toluca, Mexico*

Received 19 March 2003; accepted 8 May 2003

Abstract

The absolute differential and total cross sections for single electron capture by Ar^+ ions from Ne, Ar, Kr and Xe were measured at energies between 1.0 and 5.0 keV. For all the systems studied in this work, the reduced differential cross sections scale reasonably well with reduced scattering angle and maxima at all the collision energies studied in this work. We deduce, from the experimental differential cross section, that the electron capture channel occurs at a critical projectile-target separation of $3.25a_0$ for Ne; $3.0a_0$ for Kr and $2.89a_0$ for Xe. The total cross sections for single electron capture are compared with previous experimental measurements. These results give a general shape of the whole curve of single electron capture cross sections for the Ar^+–Ne, –Ar, –Kr and –Xe systems. Semiempirical calculations are in very good agreement with the present cross section data. It has been found that the dependence of the single electron capture cross section with the nuclear charge of the target atoms is an oscillatory function of the nuclear charge of the target atoms.

Keywords: Ar^+; Ar; Charge transfer; Angular distributions; Absolute cross sections

1. Introduction

Single electron capture by a fast ion following a collision with an atom is one of the dominant inelastic in the low-and intermediate-energy regimes and therefore these processes play a central role in the charge and energy balances of different types of plasmas, e.g., aeronomy [1] and astrophysical plasmas [2,3]. A survey of the data involving collisions of singly charged argon ions on rare gases indicates that there are few published measurements for the single electron capture cross sections for the Ar^+–Ne [4,5], Ar^+–Kr [4–8] and Ar^+–Xe [4,5] systems. Most experiments concerned with the measurement of single electron capture cross section have been performed for the Ar^+–Ar system [7–20]. Except for a few cases, the interpretation of the experimental results is based on a qualitative approach [21] to investigate the potentials of the quasi-molecular system formed in these collisions, and to examine the curve-crossing mechanism that plays such an important role in the inelastic processes. For single electron capture of Ar^+ in Ar, there is a disagreement between some of the measurements in the low keV-energy range. In this

* Corresponding author. Tel.: +52-7-29-17-59; fax: +52-7-29-17-75.
E-mail address: hm@fis.unam.mx (H. Martínez).

1387-3806/03/$ – see front matter © 2003 Elsevier Science B.V. All rights reserved.
doi:10.1016/S1387-3806(03)00263-X

work, we present absolute measurements of the differential and total cross sections for single-electron capture in Ar^+ collisions with Ne, Ar, Kr and Xe atoms, that is:

$$Ar^+ + B \rightarrow Ar^0 + \cdots,$$

where B is Ne, Ar, Kr or Xe.

The energy range covered by the present experimental study is 1.0–5.0 keV.

In addition, we present the results of the total electron capture cross section as a function of the target atomic number (Z_t) at several incident energies.

2. Experiment

Details of the experimental arrangement have been given previously [22,23], hence only a brief description of the experimental setup will be given here. Ar^+ ions were formed in a discharge source containing Ar gas (99.99% purity) at a pressure of 0.07–0.09 mTorr. Ions were extracted and accelerated in an energy range of 1.0–5.0 keV. The Ar^+ beam is passed through an einzel-type lens and directed to a Wien velocity filter in order to obtain a mass analyzed beam at the desired velocity. Next, the Ar^+ ions are passed between cylindrical electrostatic deflection plates, used both to steer the beam and to bend it by 10° to prevent photons in the ion source from reaching the detection system. Then, the collimated Ar^+ beam entered the scattering chamber, which housed a gas target cell where electron capture to form Ar^0 took place. The gas target cell was a cylinder of length 2.54 cm and diameter 2.54 cm in which the target gas pressure (typically 0.4 mTorr) was measured with a calibrated MKS capacitance manometer (model 270C). The entrance aperture was 1 mm in diameter and the exit aperture was a slit 2 mm wide and 6 mm long. This geometry permitted the measurements on the Ar^0 particles, making an angle of up to ±7° with respect to the incoming beam direction. Path lengths and apertures gave an overall angular resolution for the system of 0.1°. All apertures and slits have knife edges. The cell target was located at the center of a rotatable, computer-controlled vacuum chamber that moved the whole detector assembly, which was located 47 cm away from the target cell. A precision stepping motor ensured a high repeatability in the positioning of the chamber over a large series of measurements. The detector assembly consisted of a Harrower-type parallel plate analyzer with a 0.36-mm entrance aperture and two channel-electron multiplier (CEM) attached to its exit end. The beam entered the uniform electric field of the analyzer at an angle of 45°. The neutral beam (Ar^0) passed straight through the analyzer through a 1 cm orifice on its rear plate and impinged on a CEM so that the neutral counting rate could be measured. Separation of charged particles occurred inside the analyzer, which was set to detect the Ar^+ ions with the lateral CEM. This flux was used as a measure of the stability of the beam during the experiment. The CEMs were calibrated in situ with low-intensity Ar^0 and Ar^+ beams, which were measured as a current in a Faraday cup by a sensitive electrometer. The uncertainty in the detector calibration was estimated to be less than 4%. A retractable Faraday cup was located 33 cm away from the target cell, allowing the measurement of the incoming Ar^+ ion-beam current. A Keithley Instruments Electrometer model 610C was used to measure the beam current entering the Faraday cup. Vacuum base pressures in the system were 2.0×10^{-7} Torr without gas in the cell and 1.0×10^{-6} Torr with gas.

Under the thin target conditions used in this experiment, the differential cross sections for the formation of Ar^0 were evaluated from the measured quantities by the expression

$$\frac{d\sigma}{d\Omega} = \frac{I(\theta)}{nLI_0} \quad (1)$$

where I_0 is the number Ar^+ ions incident per second on the target; n is the number of target atoms per unit volume; L is the length of the scattering chamber, and $I(\theta)$ is the number of Ar^0 atoms per unit solid angle per second detected at a laboratory angle θ with respect to the incident beam direction. The total cross section for the production of Ar^0 was obtained by the integration of $d\sigma/d\Omega$ over all measured angles;

that is

$$\sigma = 2\pi \int_0^{0_{max}} \frac{d\sigma}{d\Omega} \sin(\theta)\, d\theta \quad (2)$$

For $\theta > \theta_{max}$, the differential cross sections drop below the experimental detection limit. If we considered this detection limit as a constant contribution for angles $\theta > \theta_{max}$, we obtained an upper limit for the estimation of this contribution for all the energies of 0.1×10^{-20} cm^{-2}, which is less than 10% for energies above 2 keV.

Extreme care was taken when absolute differential cross sections were measured. The reported value of the angular distribution was obtained by measuring it with and without gas in the target cell with the same steady beam. Then point-to-point subtraction of both angular distributions was carried out to eliminate the counting rate due to neutralization of the Ar^+ beam on the slits and those arising from background distributions. The Ar^+ beam intensity was measured before and after each angular scan. Measurements not agreeing to within 5% were discarded. Angular distributions were measured on both sides of the forward direction to assure they were symmetric. The estimated RMS error in the angular distributions is 15%, while the cross sections were reproducible to within 10% from day to day.

Several runs were made at different gas pressures and $d\sigma/d\Omega$ was determined for each run. These were compared in order to estimate the reproducibility of the experimental results as well as to determine the limits of the 'single-collision regime' since the differential and total cross sections reported are absolute.

In the present work, changes were not observed in the absolute values with respect to the ion source conditions. Also, no variation in the angular distributions were detected over a target pressure range of 0.2–0.6 mTorr.

Several sources of systematic error are present and have been discussed in a previous paper [22]. Overall uncertainties in the angular distributions were 15%, which arise from the effective length of the target cell (3%); density determination (6%), the measurement of the incident ion current (3%), and the detector calibration (3%).

3. Results and discussion

Measurements of differential cross sections (DCS) were performed at laboratory angles of $-3.6^\circ \leq \theta \leq 3.6^\circ$ and collision energies of $1.0 \leq E_{lab} \leq 5.0$ keV. Angular and energy dependencies of ρ, the reduced DCS $\rho = \theta \sin(\theta)(d\sigma/d\Omega)$ for single electron charge transfer in the laboratory system for Ar^+ on Ne, Ar, Kr and Xe are presented from Fig. 1a and d, respectively, where the abscissa is the reduced scattering angle $\tau = E_{lab}\theta$. The curves representing the reduced differential cross sections (RDCS) for the different energies scale reasonably well with τ. This is followed by a maxima and a decrease beyond 6.0, 5.0 and 4.0 keV-deg for Ar^+–Ne, –Kr and –Xe systems, respectively. At all the energies studied, $\rho(\tau)$ has a rather similar behavior within the experimental uncertainty; although for the lowest energy studied in this work (1.0 keV), the structure cannot be observed, since the largest value of τ is 3.6 keV-deg. The general behavior shows ρ to lie on a single curve that is described only by a given velocity-independent interaction potential. Each τ value thus belonging to a certain value of the collisional impact parameter b [24]. The features that occur at the same value of τ for different energies indicate that they originate at a common region of the interaction potential, since constant τ implies nearly constant impact parameter as well as constant distance of closest approach [24]. In this particular case, the impact parameter b was evaluated using an exponential shielded coulomb potential given by [24]

$$V(r) = \left(\frac{Z_p Z_t}{R}\right) \exp\left(-\frac{R}{c}\right)$$

and the reduced functions τ_0 vs. (b/c) given by Smith and co-workers [24]. The value of c was determined using the relation $c = a_0[Z_p^{2/3} + Z_t^{2/3}]^{-1/2}$, where a_0 is the Bohr radius, Z_p the projectile atomic number and Z_t the target atomic number. Since in small angle scattering, the impact parameter b and the distance

of closest approach R_0 are essentially the same, the features localized at a specific reduced angle τ_x represent interactions at some localized parts of the potential $V(r)$. In the inelastic scattering, perturbations were observed at certain localized values of τ, which provide us with knowledge of the points of the crossing of the potential curves. In the present case, our experimental results for the Ar^+–Ne system present a

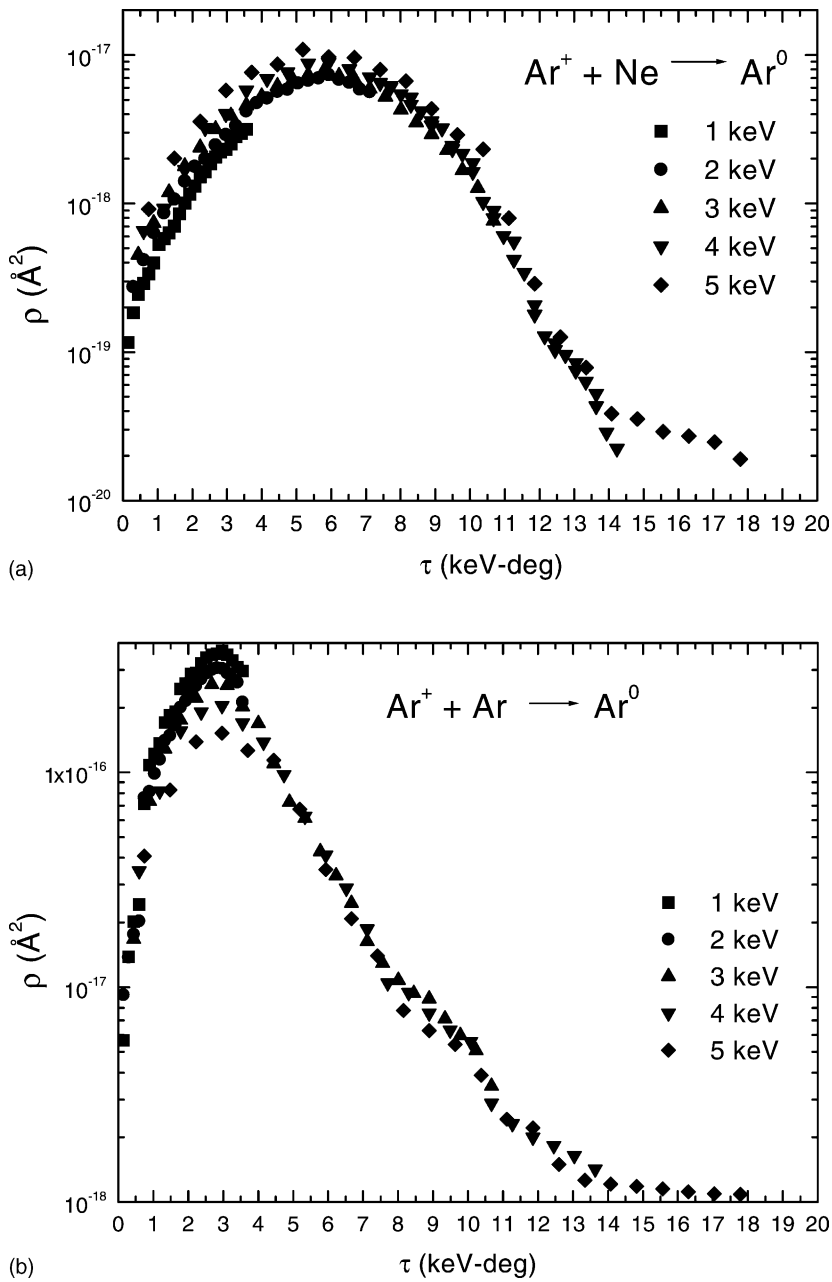

Fig. 1. Reduced differential cross sections for single-electron capture of Ar^+ ions in (a) Ne, (b) Ar, (c) Kr, (d) Xe.

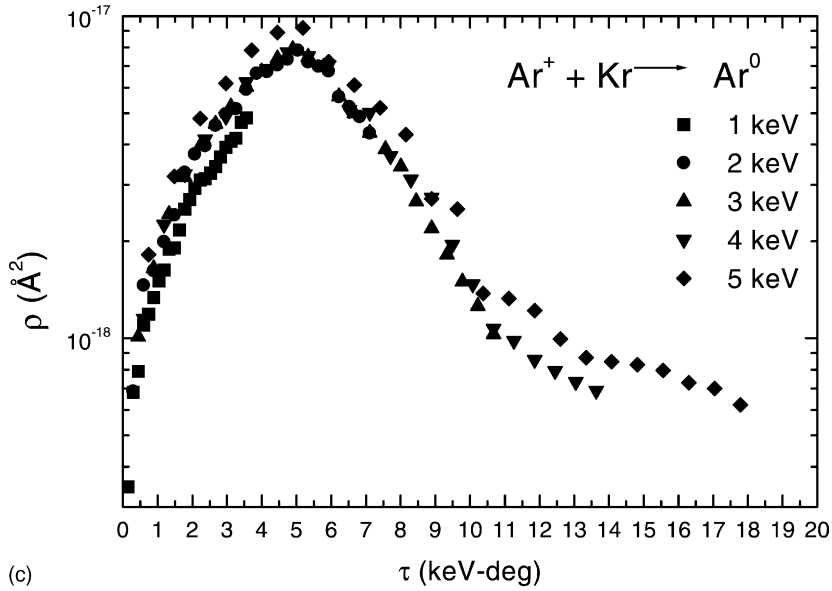

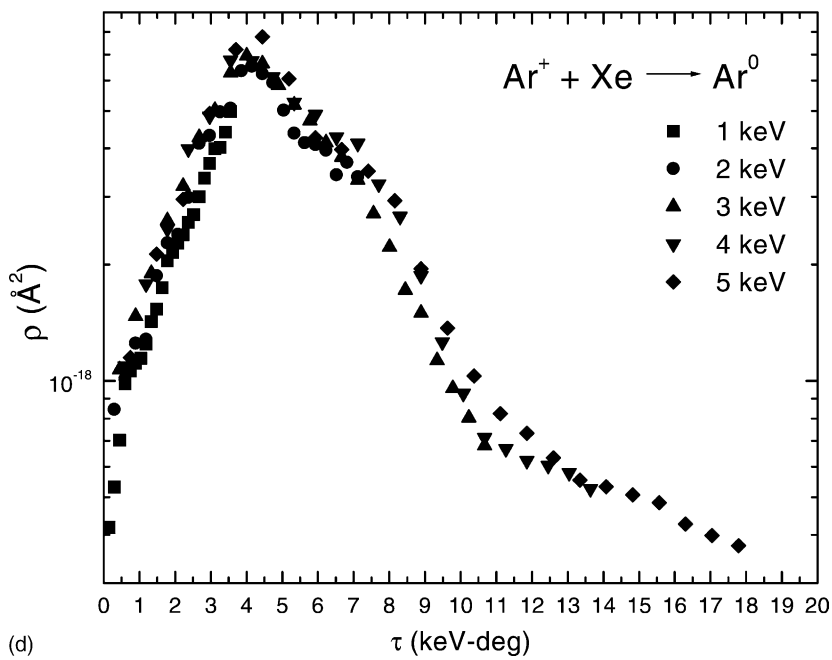

Fig. 1. (*Continued*).

maximum at 6.0 keV-deg (corresponding to the impact parameter $b = 3.25a_0$); for the Ar^+–Kr shows a maximum at 5.0 keV-deg ($b = 3.00a_0$) and the case of Ar^+–Xe system display a maximum at 4.0 keV-deg ($b = 2.89a_0$). The impact parameter estimated through the exponentially shielded coulomb potential is probably not accurate, but it is sufficient for the present purpose. These results suggest that when the Ar^+

projectile penetrates into a critical projectile-target separation (here corresponding to $b = 3.25a_0$ for Ne target; $b = 3.00a_0$ for Kr case and $b = 2.89a_0$ for Xe) the electron capture channel "opens". It is not possible at this time to identify the specific channels.

The measured differential cross sections for single electron capture of Ar^+ impacting on Ne, Ar, Kr and Xe were integrated over the observed angular range. The behavior of these data together with previous experimental data over a wide range of energy are shown in Fig. 2a and d, respectively, as a function of the incident energy. Our cross sections are found to be of the order of magnitude between 10^{-2} and 10^{-1} Å^2. Error bars are given as an indication of the maximum reproducibility of the data in the present energy range. In all cases, we have included data over a wide range of energies to show the overall shape of the curves. It can be seen from Fig. 2a for the Ar^+–Ne system that our data may connect the results at low energies of Maier [4] with those of Pivovar et al. [5] at high energies. Although there is no overlap of the three sets of data, the shapes of the cross section data of Maier [4], Pivovar et al. [5] and present measurements, indicate that the data from all three measurements are mutually consistent with the Olson model. These results give a general shape of the whole curve of the single electron capture cross sections for the Ar^+–Ne system over a wide range of energies (0.12–2000 keV). The energy dependence of the total single electron capture cross section for an Ar^+ ion colliding with Ar is shown in Fig. 2b. The shape and magnitude, within the experimental errors of the present cross sections are in very good agreement with those measured by Hegerberg et al. [15], Flaks and Solovev [20] and Fedorenko [7] and merge smoothly with the data of Jones et al. [9], Fedorenko et al. [8] and Fedorenko [7], while the magnitude of the data of Astner et al. [16], Sluyters et al. [19] and Hasted and Gilbody [18] are slightly lower but taking into the account the error bars the data are consistent with the present results.

It can be seen from Fig. 2c that the shape of the cross section for an Ar^+ ion colliding with Kr shows an increasing behavior as a function of the incident energy. Our data were found to be in good agreement with the data of Fedorenko [7] at 5.0 keV and merge smoothly into the cross sections measured by Fedorenko [7], Fedorenko et al. [8], Nikolaev et al. [6] and Pivovar et al. [5] at energies greater than 5.0 keV. While from the data of Maier [4] at low energies, it was not possible to connect with the present total cross sections. It is important to mention that the behavior of the total cross section as a function of the incident energy of the data of Maier [4] is due to that the reactants may be in excited states [4].

For Ar^+–Xe system, the total cross section shows an increasing behavior as a function of the incident energy. The present data may connect the results at high energy of Pivovar et al. [5], while the data of Maier [4] at low energies have the same order of magnitude of the present cross section. It is important to mention that the behavior of the total cross section as a function of the incident energy of the data of Maier [4] may be due to the reactants in the excited states [4].

To the best of our knowledge, no theoretical calculations are available for the non-resonant processes in order to compare with our present measurements. However, in order to obtain a preliminary understanding of the trend of the total cross sections, we considered the behavior of some of these cross sections in the intermediate energy range as illustrated in the following using the semiempirical model of Olson [25] for near-resonant charge transfer. The total single electron capture cross sections are then calculated using the universal reduced cross section of Olson [25] with the following parameters: the crossing distance R_c was taken from the experimental reduced differential cross sections; the coupling matrix element H_{12} was calculated through the expression:

$$H_{12}(R_c) = R^* \exp(-0.86R^*)$$

where $R^* = (\alpha+\gamma)(R_c/2)$. We used $\alpha^2/2$ as the effective ionization potential of the target and $\gamma^2/2$ as the ground state electron affinity [26]; and $|\Delta V'(R_c)|$ was fitted until the same value of the experimental cross section at 3.0 keV was obtained, together with the

universal reduced cross section of Olson [25]. The results of these calculations are shown in Fig. 2a, c and d as a solid line for Ar^+–Ne, –Kr and –Xe systems, respectively. Although the Olson model [25] calculation are not expected to be highly reliable, the calculation of σ_{10} seem to agree (see Fig. 2a, c and d) in shape with the measurements over the entire energy range of the present work. In these cases, it is clear that after

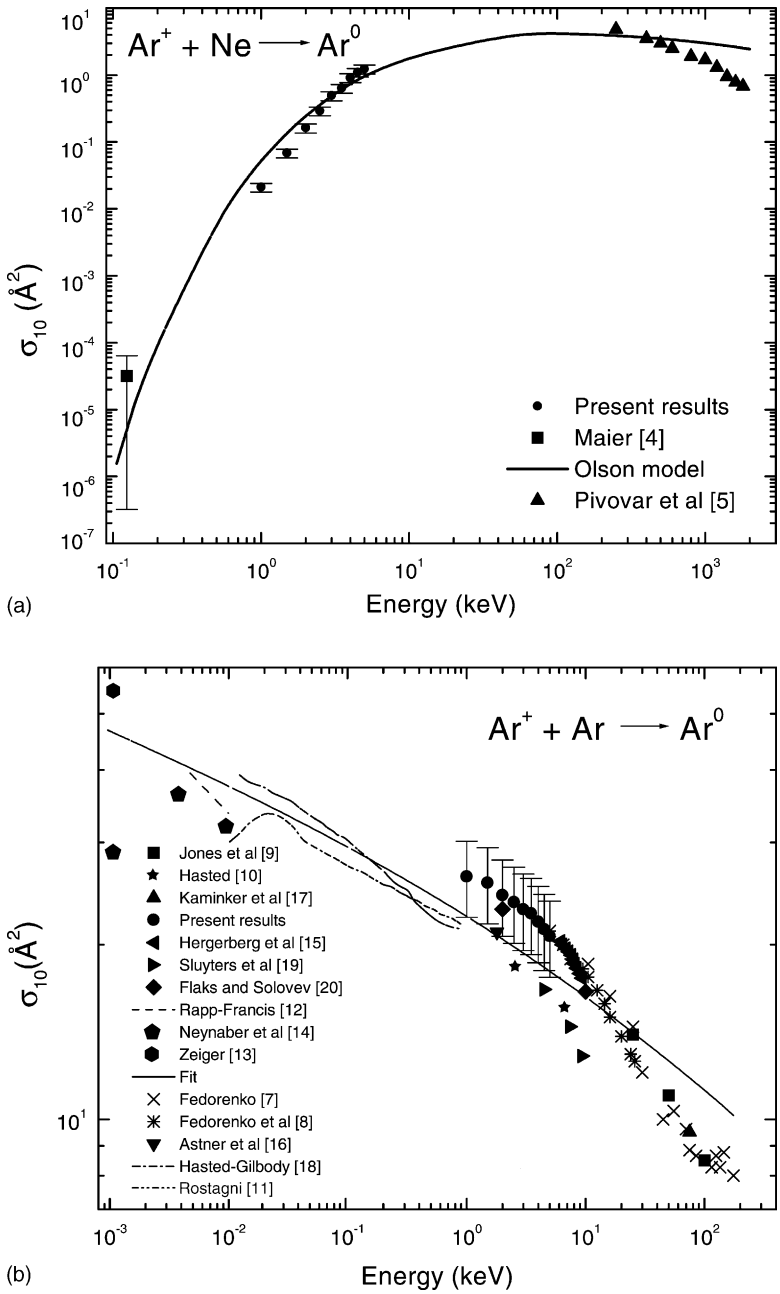

Fig. 2. Total cross sections for single-electron capture of Ar^+ ions in (a) Ne, (b) Ar, (c) Kr, (d) Xe.

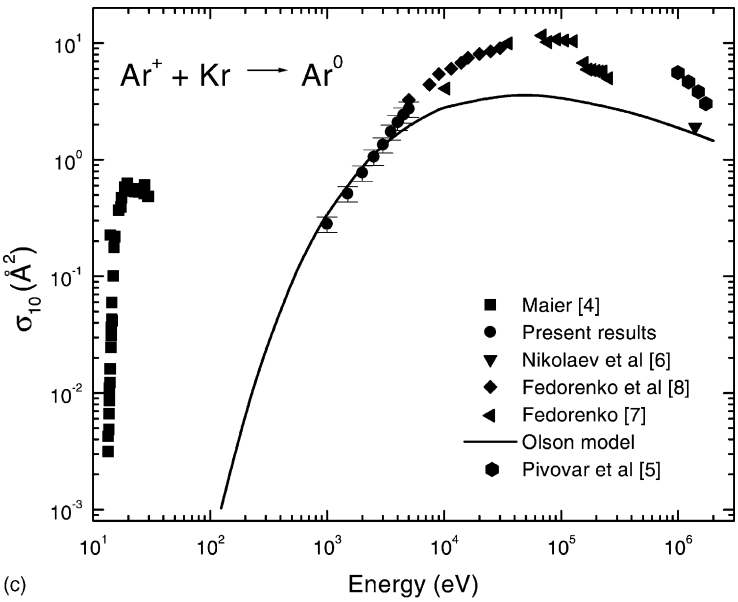

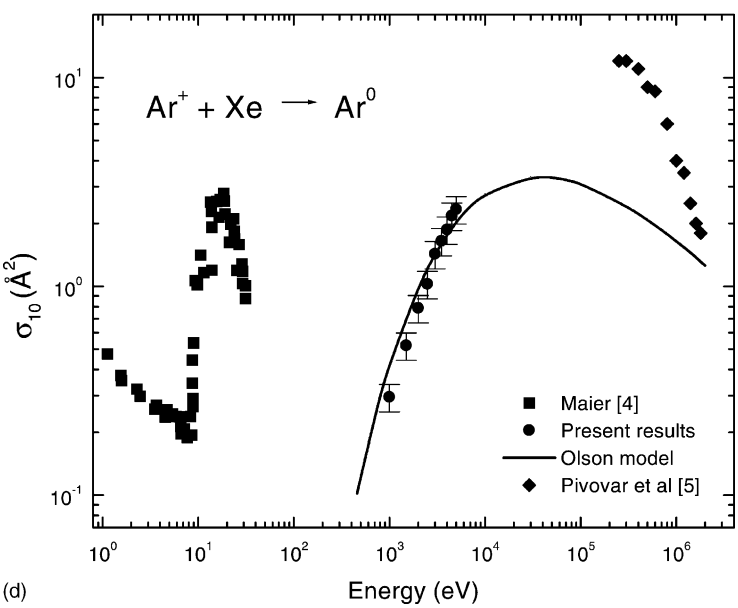

Fig. 2. (*Continued*).

fitting at 3 keV, the calculations by the Olson model reproduce the energy dependence of the cross sections well.

For the resonant system, a simple theoretical model of the process has been developed, where the results can be expressed in the form [27]:

$$\sigma^{1/2} = k_1 + k_2 \ln(E)$$

where σ is the cross section expressed in Å^2, E is the energy of the ions in keV and k_1 and k_2 are constants,

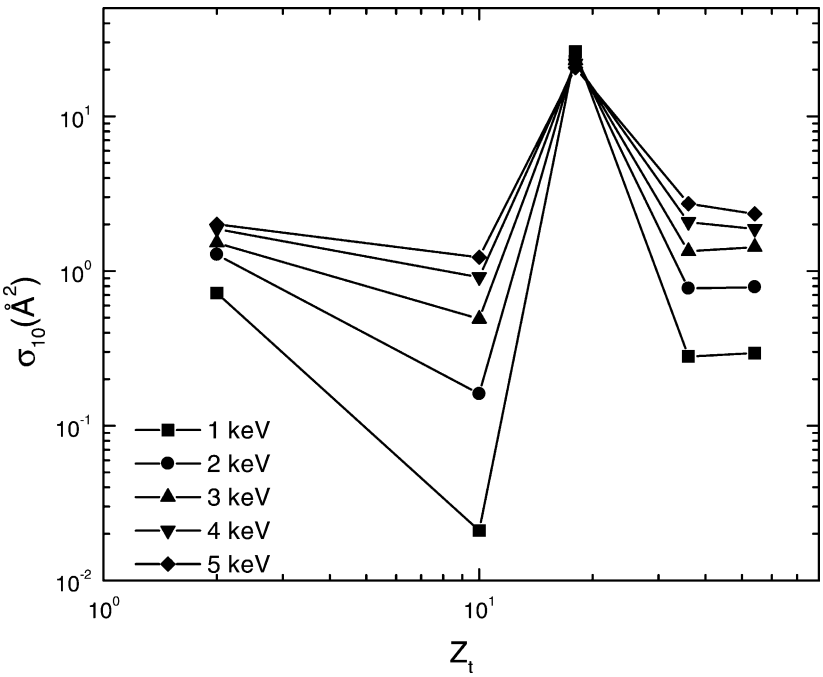

Fig. 3. Total cross sections for single electron capture of Ar^+ ions in atoms as a function of the target atomic number. Data of $Ar^+ + He$ has been taken from Martínez [22].

which are determined mainly by the ionization potential of the atom involved in the collision. The cross section function for $Ar^+ + Ar \rightarrow Ar^0$ can be represented by the expression

$$\sigma^{1/2} = [5.17 - 0.25 \ln(E)]\,\text{Å}$$

which was obtained with a least-squares fit to all the data in the energy range between 10^{-3} and 2×10^2 keV and with a correlation coefficient of 0.9872. It can be seen from Fig. 2b that the shape of the calculated cross section for an Ar^+ ion colliding with Ar shows almost the same behavior but is a factor 0.8 lower than the present values, although the agreement with previous measurements is good.

The total electron capture cross section as a function of the target atomic number (Z_t) for laboratory energies between 1.0 and 5.0 keV is shown in Fig. 3. All the curves display the same oscillatory behavior having a cross section minimum (within the resolution in Z_t) at $Z_t = 10$, followed by a common maximum at $Z_t = 18$, following an experimental evidence of a smooth dependence for higher Z_t values, for all the energies studied in this work. An analogous oscillation in the dependence of the cross sections on the nuclear charge Z_t of the target atoms was previously observed by Dimitriev et al. [28], Bell and Betz [29] and Martínez et al. [30]. Bell and Betz [29] calculated the cross section for electron capture to the K shell of Cl ions with an energy of 120 MeV using the Brinkman–Kramers formula and found a non-monotonic dependence on Z_t. Dmitriev et al. [28], point out that this phenomenon is caused by the analogous oscillations of the values of the equilibrium charge fraction and the average charge of the fast ions, which arise as a consequence of the shell structure of the atoms. The present experimental results confirm the prediction of the Oppenheimer–Brinkman–Kramers calculation which states that the oscillations in the capture cross sections must also be observed at velocities down to v–v_0 ($v_0 = 2.18 \times 10^8$ cm).

4. Conclusions

We have presented values of absolute differential and total cross sections for single electron capture by Ar^+ from Ne, Ar, Kr and Xe at impact energies between 1.0 and 5.0 keV. The results of the present work can be summarized as follows: (a) the reduced differential cross sections scale reasonably well with τ. This is followed by structure and a decrease beyond 6.0, 5.0 and 4.0 keV-deg for Ar^+–Ne, –Kr and –Xe systems, respectively. (b) These results suggest that when the Ar^+ projectile penetrates into a critical projectile-target separation (here corresponding to $b = 3.25a_0$ for Ne target; $b = 3.00a_0$ for Kr case and $b = 2.89a_0$ for Xe) the electron capture channel "opens". (c) The total cross sections for single electron capture are compared with previous experimental measurements. These results give a general shape to the whole curve for the single electron capture cross sections. (d) Semiempirical calculations are in good agreement with present cross sections data. (e) We show the single electron capture cross section of Ar^+ ions on various atoms and the oscillatory dependence of the single electron capture cross section on the nuclear charge of the target atoms.

Acknowledgements

We are grateful to F.B. Yousif for helpful suggestion and comments, and thank José Rangel, A. González and A. Bustos for their technical assistance. This work was supported by DGAPA IN-100392 and CONACyT 41072-F.

References

[1] G. Siscoe, Rev. Geophys. 33 (1995) 519.
[2] J.S. Kaastra, Hot Universe 188 (1998) 43.
[3] C. Uberoi, Pramana-J. Phys. 55 (2000) 645.
[4] W.B. Maier II, J. Chem. Phys. 69 (1978) 3077.
[5] L.I. Pivovar, M.T. Novikov, M. Tubaev, Sov. Phys. JETP 19 (1964) 318.
[6] V.S. Nikolaev, I.S. Dmitriev, L.N. Fateeva, Y.A. Teplova, Sov. Phys. JETP 13 (1961) 695.
[7] N.V. Fedorenko, J. Tech. Phys. (USSR) 24 (1954) 2113.
[8] N.V. Fedorenko, V.V. Afrosimov, D.M. Kaminker, Sov. Phys. JETP 1 (1956) 1861.
[9] P.R. Jones, F.P. Ziemba, H.A. Moses, E. Everhart, Phys. Rev. 113 (1959) 182.
[10] J.B. Hasted, Proc. Roy. Soc. London A205 (1951) 421.
[11] A. Rostagni, Nuovo Cim. 12 (1935) 134.
[12] D. Rapp, W.E. Francis, J. Chem. Phys. 37 (1962) 2631.
[13] A. Zeigler, Z. Phys. 136 (1953) 108.
[14] R.H. Neynaber, S.M. Trujillo, W. Rothe, Phys. Rev. 157 (1967) 101.
[15] R. Hegerberg, S. Thórarinn, M.T. Elford, J. Phys. B11 (1978) 133.
[16] G. Astner, A. Bárány, H. Cederquist, H. Danared, S. Huldt, P. Hvelplund, A. Johwson, H. Knuden, L. Liljeby, K.G. Rensfelt, J. Phys. B: At. Mol. Phys. 17 (1984) L877.
[17] D.M. Kaminker, N.V. Fedorenko, Zh. Tekh. Fiz. 25 (1955) 2239.
[18] J.B. Hasted, H.B. Gilbody, Proc. R. Soc. A238 (1956) 334.
[19] J.M. Sluyters, E. de Haas, J. Kistemaker, Physica 25 (1959) 1376.
[20] J.P. Flaks, E.S. Solovev, Sov. Phys.-Tech. Phys. 3 (1958) 564.
[21] V. Sidis, M. Barat, D. Dhuicq, J. Phys. B8 (1975) 474.
[22] H. Martínez, J. Phys. B: At. Mol. Opt. Phys. 31 (1998) 1553.
[23] H. Martínez, Phys. Rev. 63 (2001) 042702.
[24] (a) F.T. Smith, R.P. Marchi, K.G. Dedrick, Phys. Rev. 150 (1966) 79;
(b) F.T. Smith, R.P. Marchi, W. Berth, D.C. Lorents, Phys. Rev. 161 (1967) 131.
[25] R.E. Olson, Phys. Rev. A2 (1970) 121.
[26] E.W. McDaniel, Atomic Collisions, Wiley, New York, 1989, p. 656.
[27] S. Sinha, J.N. Bradsley, Phys. Rev. A14 (1976) 104.
[28] I.S. Dimitriev, N.F. Vorobiev, V.P. Zaikov, Z.M. Konovalova, V.S. Nikolaev, Y.A. Teplova, Y.A. Fainberg, J. Phys. B: At. Mol. Opt. Phys. 15 (1982) L351.
[29] F. Bell, H.D. Betz, J. Phys. B: At. Mol. Opt. Phys. 10 (1977) 483.
[30] H. Martínez, P.G. Reyes, J.M. Hernández, B.E. Fuentes, Int. J. Mass Spectrom. 198 (2000) 77.